Journal of the Korean Nuclear Society
Volume 17, Number 2, June 1985

A Mechanistic Model for In-Reactor Densification of UO_2

Woan Hwang, Keum Seok Seo and Ho Chun Suk
Korea Advanced Energy Research Institute
(Received April 10, 1985)

UO_2 핵연료의 노내 기계론적 고밀화 모형

황 완·서 금 석·석 호 천
한국에너지연구소
(1985. 4. 10 접수)

Abstract

Considering vacancy generation and migration in grain and sink at grain boundary, a mechanistic densification model which is dependent on UO_2 temperature and microstructure has been developed. This densification model is a function of time, fission rate, temperature, density, pore size distribution and grain size. The resultant equation derived in this model which is different from Assmann and Stehle's resultant equations for four temperature regions, can be applied directly for all the pellet temperatures. The predictions of the present densification model very well agreed with the experimental data. This model well predicts absolute magnitude and trend in comparison with the empirical algorithm used in KFEDA code.

요 약

본 논문에는 이산화 우라늄 소결체의 노내고밀화현상을 온도와 미세구조의 함수로 정확하게 예측할 수 있는 기계론적 이론 모형이 개발·기술되어있다. 이 모형은 UO_2 소결체의 결정입계내에서 공극(vacancy)이 생성 이동되고, 결정입계에서 공극이 소멸되는 현상을 고려하고 있으며, 이 과정에서 일어나는 고밀화의 크기가 핵분열율, 조사시간, UO_2 소결체밀도, 기공 크기의 분포, 결정입크기 및 온도의 함수로 기술되어 있다. 본 모형의 기공 수축에 대한 결과식은 Assmann과 Stehle가 유도한 4개의 온도 영역에대한 결과식과는 상이한 것으로서, 소결체의 모든 온도 영역에 직접 적용된다.

본 모형에 의한 노내고밀화 크기의 예측치는 실험자료와 아주 잘 일치하며, KEFDA 전산코드에 사용된 경험적 실험 연산식에 비하여 고밀화의 경향과 절대치를 보다 정확히 예측한다.

Nomenclature

a	lattice constant of UO_2
C	local vacancy concentration
Ci	equilibrium vacancy concentration
Cs	saturation concentration of vacancies in UO_2
C_T	thermal vacancy concentration
γ	surface tension of UO_2
D	self-diffusion coefficient of uranium in UO_2
D_v	vacancy diffusion coefficient
D_v^{th}	thermal vacancy diffusion coefficient

D_v^{irr} irradiation induced vacncy diffusion coefficient
$\Delta\varepsilon$ gain of surface energy
$(\Delta V/V_0)^c$ relative volume change due to coarse porosity densification
$(\Delta V/V_0)^f$ relative volume change due to fine porosity densification
$\Delta V/V_0|_t$ total relative volume change due to swelling and densification
η fraction of vacancies
F fission rate
g numerical parameter
k Boltzmann constant
λ fission spike length
ν vibration frequency of the uranium atom
P local porosity
P, P_o, P_{oi} porosity, initial porosity, initial porosity in the i_{th} pore class
P_o^f fraction of fine porosity
P_o^c fraction of coarse porosity
Q_s threshold energy
Q_F energy of vacancy formation
Q_M energy of vadancy migration
r, r_o, r_{oi} pore radius, initial pore radius, initial pore radius in the i_{th} pore class
r_g, r_{go} grain radius, initial grain radius
r_c radius of coarse pores
r_p radius of fine pores
t time
T temperature
t_{oi} time for the i_{th} pore class to disappear
Z_c density of coarse pores
Z_p density of fine pores
ω UO_2 volume(5×10^{-19} cm^3)
Ω vacancy volume
Ω_s fission spike volume

1. Introduction

Thermal reactor fuel pellets are manufactured with a small percent of residual porosity to accommodate the swelling caused by solid fission products during irradiation and to trap some of the gaseous fission products[1]. In-reactor densification[2,3] doesn't present an operating problem in CANDU-PHWR(Canadian Deuterium Uranium-Pressurized Heavy Water Reactor) UO_2 fuel because of design features such as short(50mm) elements, collapsible sheathing, high-density pellets, and horizontal configuration. However, allowance for densification permits a more accurate calculation of changes in fuel porosity and, subsequently, fuel thermal conductivity, gap conductance, fuel temperature, dimensional change of fuel, fission gas release, and stored energy. Since many of the fuel behaviours are sensitive to temperature, it is important to be able to predict the extent of densification with confidence under a wide range of operating conditions.

Densification is defined as in-reactor volume changes of the UO_2 without stress from external forces. Out-reactor thermal sintering in UO_2 occurs only to a measurable extent at temperature in excess of 1200°C, but in-reactor densification was found at temperature as low as 400°C[3,4]. In both cases, however, densification is caused by pore shrinkage and disappearance of pores, which are typical for the final stage sintering. Coble[4] treated, at first, the thermal sintering kinetics for the intermediate and final stage as a vacancy diffusion model.

Marlowe[6] used Coble's theory of the final stage of sintering which is based on the dependence of density increase on grain growth. Marlowe replaced the thermal diffusion coefficient by an irradiation induced athermal diffusion coefficient. The magnitude was determined in experiments on irrdiation-induced densification. Some authors utillized Marlowe's formula and fitted the containing parameters with respect to the measred values of densification[3,6,7]. Zimmerman[8] calculated the densification on the basis

of irradiation-induced vacancy generation and their annihilation at dislocation.

MacEwen and Hastings[9] who considered Marlowe's theory to be incorrect assumed that pore shrinkage is caused by the different trapping probabilities of vacancies and interstitials at pores, grain boundaries, and dislocations. They derived the detailed models based on above phenomena, using rate-theory equations. But their models required the simultaneous solution of 17 non-linear differential equations which calculate how the sintering pore size distribution changes with time. Speight[1,10] criticized MacEwen and Hastings's concept, pointing out that the model described only a redistribution of pore volume within the grain which results in an insignificant densification of about 0.02% under irradiation conditions. That is, whereas absorption of interstitial atoms can lead to void shrinkage, the free vacancies can not reach grain boundaries at thermal reactor temperatures and hence the over-all pellet density can increase only to a very limited extent by lattice relaxation. It is likely that an irradiation-enhanced diffusion coefficient would give more plausible results but the model does not cater for this. Speight reproduced almost exactly the calculations of vacancy and interstitial concentration through the life but showed that, even if one assumes that pores are traps only for interstitials, the total decrease in void volume can only be 0.04% compared with MacEwen and Hastings[2] value of 1.4%. Thus, an initial void volume of 3% is changed negligibly to 2.96%. Since $\Delta\Omega/\Omega$ may be expected to be within the range 1/3 to 1/2, the accompanying density increase is in a range from 0.013 to 0.02% [10], where $\Delta\Omega/\Omega$ is the fractional volume relaxation around a single vacancy.

Dollins and Nichols [1,11,12] proposed a mechanistic model with a different description of intragranular and intergranular porosity. In the first case, irradiation induced generation of vacancies and interstitials at pores and in the lattice is taken into account. And trapping of vacancies at dislocation, pores, damage cascades and grain boundaries is considered. Also, recombination and trapping of fission gas atoms by pores and their resolution are taken into account. In the second case, densification is described in terms of thermal and irradiation-induced generation and annihilation of vacancies, grain boundary diffusion, and trapping of fission gas atoms.

In recent years, a number of empirical and mechanistic models have been developed. Current modelling of densification consists of empirical expressions derived mostly from measuremets of pellet bulk density and mechanistic models based on theoretical arguments. The empirical models may be applicable only for one fuel type operating under the irradiation conditions for which the expression was fitted. Also empirical correlations do not provide a simple method of representing changes in pore size spectra during in-reactor densification. A model developed by Stehle and Assmann[13] can be characterized by a two-step mechanism: (i) generation of an excess vacancy concentration around the pores and (ii) partial migration of these vacancies to the grain boundries. The mechanistic models have not been fully evaluated yet because of a lack of experimental data of the required quality.

We developed, so-called, KFMD(KAERI Fuel Mechanistic Densification) model, considering vacancy generation and migration in grain, which was considered also in the Assmann and Stehle's model. Some parts of the Assmann and Stehle's resultant relationships were based on fault assumptions which is a discontinuty in the function of remaining porosity as temperature. This phenomenon is physically unaccetpable. Also, Assmann and Stehle's fine pore model did not consider the trapping of the vacancies by coarse pores and the growing of the coarse

pore. Therefore, in this report, some modifications were made to Assmann and Stehle's modelling of coarse pores and their fine pore model. In order to calculate a shrinkage rate of coarse pore, ZERO function[25] was developed in this study. The in-reactor changes in size of sintered UO_2 pellet are analyzed by superimposing matrix swelling and pore shrinkage. At first, pore shrinkage dominates and results in densification, an effect which has been known. With regard to shrinkage mechanism one should distinguish between very fine pores and coarse pores; the latter being responsible for the majority of total porosity in well sintered UO_2 pellet. The total porosity was subdivided into several pore size classes, ranging from submicroscopic pores to those visible in the microscopic range, which were treated separately. For the coarse porosity, a two-step process was postulated; first, the generation of vacancies by the fission fragments transversing the pore, second, the migration of these vacancies to effective sinks (grain boundaries). Densification rate equations for all temperature regions were then derived, and a quadratic-resultant equation for the coarse porosity was drived.

2. Derivation of the General Rate Equation for In-reactor Pore Shrinkage of Coarse Pores

Densification is, in principle, a two-step mechanism: (1) generation of an excess vacancy concentration around the pores, and (2) partial migration of these vacancies to the grain boundaries. We consider that: first, generation and reabsorption of single vacancies at or close to the surface of the pore, second, migration of excess vacancies to the grain boundary.

The number of vacanies, Z^+, generate per time unit is given by[13]

$$Z^+=\frac{8\pi r^2\nu}{a^2 g}e^{-Q_s/KT}(1-Ci)+\frac{4\pi r^2}{3}\lambda F\frac{\omega}{\Omega}(C_s-C_i) \quad (1)$$

The first term in Eq. (1) describes the vacancy generation rate by thermal activation, where $4\pi r^2$ is the surface area of the pore, $a^2/2$ is the surface area per atom, a is the lattice pameter and ν is vibration frequency. In principle, the parameter $g(>1)$ takes into account that more than one jump is necessary to transport a vacancy to the place which the concentration is C_i. Ci is the equilibrium vacancy concentration close to the pore surface where the fisson induced vacancies are generally implanted. Qs is a threshold energy with $Qs\simeq Q_F+Q_M$, where Q_F is the energy of vacancy formation and Q_M is the energy of vacancy migration. The second term in Eq. (1) describes the vacancy generation rate by fission spikes. In this term, $(4\pi r^2/3)\ \lambda F$ is the number of encounters of a fission spike with a pore per unit time[13,14], λ is spike length, F is the volumetric fission rate, and $\omega(C_s-C_i)$ is the volume which is effectively converted into vacancies by one event, Ω is the vacancy volume and Cs is the saturation concentration of vacancies in UO_2. The number of vacancies, Z^-, which are reabsorbed by the pore per unit time is given by

$$Z^-=\frac{8\pi r^2}{a^2}\ \frac{\nu}{g}\exp\{-(Q_s-Q_F+\Delta\varepsilon)/KT\ C_i\} \quad (2)$$

where $\Delta\varepsilon=(2\gamma/r)\Omega$ is the change in gain of surface energy. If a certain pore absorbs one vacancy, the volume of the pore is increased and the surface energy of the pore is increased. The surface energy of pore is $2\gamma/r$ where γ is the surface tension.

The behaviour of the vacancy diffusion is described by Fick's first law of diffusion

$$J_v=-D\frac{dC}{dx} \quad (3)$$

J_v is the number of vacancies diffusing down

the concentration gradient per second per unit area; it is termed the flux of vacancies. C is the concentration of vacancies. D is the diffusion cofficient ($cm^2\ s^{-1}$). Therefore, the vacancy migration flux J_v is given by

$$J_v = -(D_v^{th} + D_v^{irr}) \cdot \frac{dC}{dx} \tag{4}$$

A concentration gradient will be established which will, in turn, produce a counterflow in accordance with the usual Fick's law, where the concentration gradient of vacancy is given by

$$\frac{dC}{dr} = \frac{C_i - C_T}{r_g - r} \cdot (4\pi \cdot r_g \cdot r) \tag{5}$$

where, r_g is the radius of grain and
r is the radius of pore

The number of vacancies, migrating from the pore to the grain boundary, can be obtained as dividing the flux J_v by unit vacancy volume, Ω. Therefore, if we substitute Eq. (5) into Eq. (4) and divide by the volume of a unit vacancy, we obtain the following eqution.

$$Z_m = \frac{4\pi (D_v^{th} + D_v^{irr})}{\Omega} (C_i - C_T) \frac{r_g \cdot r}{r_g - r} \tag{6}$$

Where Z_m is the number of vacancies, migrating per unit time from the pore with radius r to the sink (grain boundary) where D_v^{th} and D_v^{irr} are the thermal and irradiation induced vacancy diffusion coefficient respectively, and C_T is the thermal vacancy concentration at the sink. The pore volume decreases according to $dv/dt = -Z_m\Omega$. With $dv = 4\pi r^2\, dr$, we obtain the following rate equation for the shrinkage of the pore radius:

$$\frac{dr}{dt} = -(D_v^{th} + D_v^{irr})(C_i - C_T) \frac{r_g}{r(r_g - r)} \tag{7}$$

Since $Z_m = Z^+ - Z^-$ under equilibrium conditions, $(C_i - C_T)$ can be calculated from Eq. (1), (2) and (6):

$$C_i - C_T = \left[\frac{2\nu\Omega}{a^2} e^{-Q_i/KT} \frac{1}{g} \{1 - C_T(1 + e^{Q_F/KT} e^{-\Delta\varepsilon/KT})\} + \frac{\lambda\omega F}{3}(C_s - C_T) \right] /$$
$$\left[\frac{2\nu\Omega}{a^2} e^{-Q_i/KT} \times \frac{1}{g} \{1 + e^{Q_F/KT} e^{-\Delta\varepsilon/KT}\} + \frac{\lambda\omega F}{3} + \frac{(D_v^{th} + D_v^{irr}) r_g}{r(r_g + r)} \right].$$

With $e^{-\Delta\varepsilon/KT} \simeq \left(1 - \frac{2}{rKT}\right)$ and $C_T = e^{-Q_F/KT}$, and considering the order of magnitude relationships among the different terms in Eq. (8), we obtain the following relationship:

$$C_i - C_T = \frac{\frac{2\nu\Omega}{a^2} e^{-Q_i/KT} \frac{1}{g} \frac{2\gamma\Omega}{rKT} + \frac{\lambda\omega F}{3}(C_s - C_T)}{\frac{2\nu\Omega}{a^2} e^{-(Q_i - Q_F)/KT} \frac{1}{g} + \frac{\lambda\omega F}{3} + \frac{(D_v^{th} + D_v^{irr}) r_g}{r(r_g - r)}} \tag{9}$$

With the relationship

$$D_v^{th} = a^2 \nu e^{-(Q_i - Q_F)/KT}$$

and $\Omega = a^3/4$ for *fcc* lattice[24], we obtain

$$C_i - C_T = \frac{D_v^{th}\ C_T \frac{1}{ga} \frac{\gamma\Omega}{rKT} + \frac{\lambda\omega F}{3}(C_s - C_T)}{D_v^{th}\ \frac{1}{2ga} + \frac{\lambda\omega F}{3} + \frac{(D_v^{th} + D_v^{irr}) r_g}{r(r_g - r)}} \tag{9-1}$$

where the UO_2 self-diffusion coefficient D is given by

$$D = a^2 \nu e^{-Q_i/KT} = a^2 \nu e^{-Q_i/KT} (e^{Q_F/KT})(e^{-Q_F/KT}) = D_v^{th} \cdot C_T$$

If we substitute Eq. (9-1) into Eq. (7), we obtain the final rate equation for the shrinkage of the pore radius:

* The surface area per unit cell is $6a^2$. In the case of a *fcc* lattice, each unit cell has 12 atoms. Therefore, the surface area per atom is $a^2/2$.

$$\frac{dr}{dt}=-\frac{(D_v^{th}+D_v^{irr})r_g}{r(r_g-r)}\times\frac{\frac{\gamma\Omega D}{rKt}\frac{1}{ga}+\frac{\lambda\omega F}{3}(C_s-C_T)}{D_v^{th}\frac{1}{2ga}+\frac{(D_v^{th}+D_v^{irr})r_g}{r(r_g-r)}+\frac{\lambda\omega F}{3}} \tag{10}$$

3. Evaluation of Assmann's Modelling of Coarse Pore

The rate Eq. (10) of Assmann can, in general, only be solved by numerical methods. As shown in Fig. 1, the logarithmic plot of the pore shrinkage rate versus the reciprocal temperature clearly resolves into four separate temperature regions. The slope in region IV corresponds to the activation energy for the self-diffusion coefficient of UO_2. The slope in region Ⅱ reflects the activation energy of vacancy migration coefficient, which amounts to about half of the activation energy of self-diffusion. Region Ⅲ is characterized through a plateau; its level depends upon the fission rate. In order to make the rate Eq. (10) of Assmann easy to describe, it can be abbreviated by

$$\frac{dr}{dt}=-A\frac{B+C}{D+A+E} \tag{11}$$

where $A=\frac{(D_v^{th}+D_v^{irr})r_g}{r(r_g-r)}$

$$B=\frac{\gamma\Omega D}{rKTga}$$

$$C=\frac{\lambda\omega F}{3}(C_s-C_T)$$

$$D=\frac{D_v^{th}}{2ga}$$

$$E=\frac{\lambda\omega F}{3}$$

Here, A involves the thermal and irradiation induced vacancy diffusion coefficient and geometrical aspects. B and D represent mainly the contribution from the thermal process. C and E represent the athermal contribution from the fission spikes. Assmann assumed that the rate Eq. (11) can be simplified in the distinct temperature regions Ⅰ, Ⅱ, Ⅲ and Ⅳ due to specific order of magnitude relationships among A, B, C, D and E. Taking into account an appropriate description of the pore structure and integrating the simplified equations for the pore shrinkage rate, Assmann obtained relationships for the densification kinetics in the particular temperature regions. However, as shown in Fig. 2, discontinuities exist when Assmann's equations

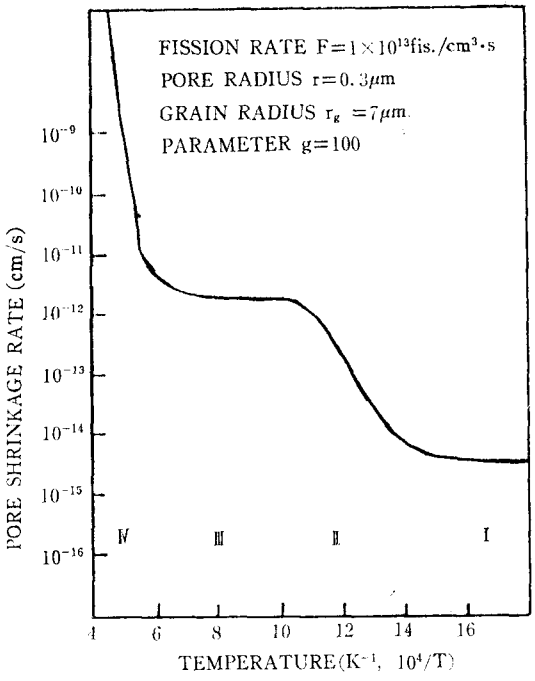

Fig. 1. Arrhenius Plot for the Pore Shrinkage Rate (Coarse Pores)

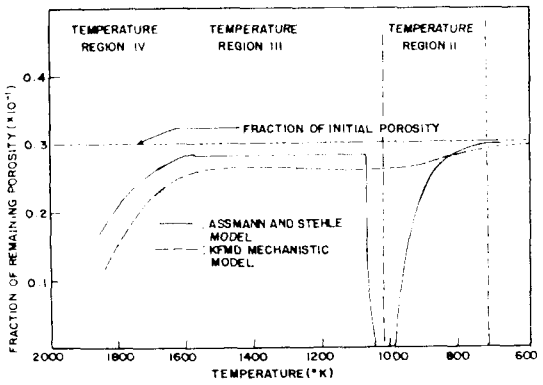

Fig. 2. Distribution of Remaining Porosity at Burnup 40 MWH/KGU

are applied in four separate temperature regions.

1) Regions I and II

Assmann assumed that, since at low temperature (<450°C) and moderately low temperatures (between about 450 and 750°C), A, C and E dominate over B and D, and if $r \ll r_g$, Eq. (11) can be reduced to

$$\frac{dr}{dt} = -A\frac{C}{E} = -(D_v^{th} + D_v^{irr})C_s \frac{1}{r} \qquad (12)$$

where C_T has been neglected, because $C_T \ll C_s$.[13] C_s is the limiting vacancy concentration in the matrix. If we integrate Eq. (12) and sum over all pore classes with initial radius, r_{0i} and the pore volume fraction, p_{0i}^c. The resultant equation should be

$$\left(\frac{\Delta V}{V_0}\right)^c = -\sum_i P_{0i}^c \left[1 - \left\{1 - \frac{2(D_v^{th} + D_v^{irr})C_s \cdot t}{r_{0i}^2}\right\}^{3/2}\right] \quad (13)^*$$

and the pore disappearance time, t_{0i}, is given by

$$t_{0i} = \frac{1}{2(D_v^{th} + D_v^{irr})C_s} r_{0i}^2 \qquad (14)^*$$

As shown in Fig. (3), Eq. (13) may be satisfied for region I, but D term of rate Eq.(11) cannot be neglected in region II, as the effect of D term is larger than that of C term. If we use the Eq. (13), we can find a discontinuity in the boundary between region II and region III, as shown in Fig. 2.

2) Region III

As shown in Fig. 1, region III is characterized by a plateau whose level depends upon the fission rate. Assmann assumed that at moderately high temperature (between about 750°C and 1,300°C) the terms A, C and D in rate Eq. (11) are dominant. If again $r \ll r_g$ and since $C_T \ll C_s$, Eq. (11) can be simplified to

$$\frac{dr}{dt} = -A\frac{C}{A+D} = -\frac{\lambda F \omega}{3\beta} C_s \qquad (15)$$

with $\beta = (1 + r/2ag)$. In the case $\beta \simeq 1$, we obtain

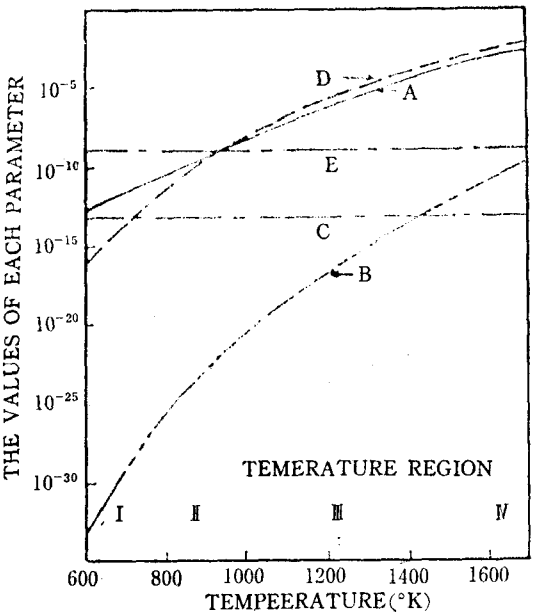

Fig. 3. Sensitivity of Each Parameter A,B,C,D and E

$$\frac{dr}{dt} = -\frac{\lambda F \omega}{3} C_s \qquad (15\text{-}1)$$

In Eq. (15), Assmann assumed $\beta = (1 + r/2ag) \simeq 1$ which mean $r \ll ag$. Since $ag \simeq 0.05\mu m$, the radius of pores has to be less than $0.05\mu m$ which is the radius for a fine pore and not a coarse pore.* Even so the E term is neglected and the resultant equation in region III should be changed as follows;

$$\left(\frac{\Delta V}{V_0}\right)^c = -\sum_i P_{0i}^c \{1 - (1 - \text{DISTIME})^3\} \qquad (16)$$

where

$$\text{DISTIME} = 1 - \frac{[\{-\frac{4}{3}(ag\lambda F\omega C_s)t + (r_0 + ag)^2\}^{1/2} - 2ag]}{r_0}$$

Even more, E term shall not be neglected either as the densification level depends upon the fission rate and the magnitude of E term is larger than that of C term. If E term is neglected, this equation reduces to an equation

* In original Assmann's paper (Ref. 13), the factor 2 is missed.

* The radius of coarse pore is usually considered larger than $0.5\mu m$[13]

which can be used only for out-of-pile densification.

We found that there were some mistakes in Assmann's resultant equations. Also, we can see that there are major assumptions when the equations are developed in temperature region I ~ III. As shown in Fig. (2), we can find discontinuties in regions I and II. Therefore, we must not use these resultant Eqs. (13) and (16) in order to calculate the fraction of the remaining pores by pore shrinkage under irradiation condition. Hence, the calculational method of section 4 is recommended.

4. The Calculational Method for the General Rate Equation

As a result evaluated in section 3, we can see that the resultant simplified equations integrated at each of the temperature regions cannot be applied, as some factors had been neglected in Eqs. (12) and (15). First of all, we find some discontinuities at the boundaries of each of temperature regions. Nevertheless, the qualitative results ,i.e., trends, agree with experimental results in temperature regions III and IV but the quantitative results did not agree with experimental results.

The densification rate for temperature region III is larger than that at the end the region IV (~1300°C). However, we cannot integrate the rate equation exactly in the temperature regions I,II and III because the terms A,B,C,D & E in Eq. (11) have complicated relations with each another. Therefore, we have need to use the rate equation directly in all temperature regions. If we use the general rate Eq. (10) directly, in general, it can only be solved by numerical methods but requires too much calculation time. Therefore, the following integration method is developed and recommented.

4.1 The Integration Method of the Rate Equation

In order to provide reliable predictions of the changes in pore size distribution, the basic mechanisms must be physically followed and, in addition, there is an incentive to keep the model as simple and easy to apply as possible.

The initial intragranular porosity can be divided into two groups such as fine pores and coarse pores. The coarse porosity can be further characterized by five size ranges, such as used in this work. Coarse pores keep their identity and show a continuous shrinkage of the pore radius. For this reason, fission-induced fuel density changes can be described for pores only by equations for average porosity, whereas the behaviour of coarse pores can be described by an equation for the individual pore radii.

To calculate how the sintering pore size distribution changes with time and power requires the solution of the non-linear differential Eq. (10).

For $r \ll r_g$, and $C_T \ll C_S$, Eq. (10) can be simplified to

$$\frac{dr}{dt} = -\frac{D_v}{r} \times \frac{\frac{S}{r} + Z}{\frac{D_v}{r} + B} \tag{17}$$

where

$$B = \frac{D^v_{th}}{2ag} + \frac{\lambda \omega F}{3}$$

$$Z = \frac{\lambda \cdot F \cdot \omega \cdot C_S}{3}$$

$$D_v = D_v^{th} + D_v^{irr}$$

$$S = \frac{\gamma \Omega D}{KTag}$$

B, Z, D_v and S are constants. Eq. (17) can be simplified again to yield

$$\frac{dr}{dt} = -\frac{D_v(S+Zr)}{r(D_v+Br)} \tag{18}$$

In order to integrate Eq. (18) from r_0 to r_1, we can rearrange the Eq. as follows

$$\int_{r_0}^{r_1} \frac{r\left(1+\frac{Br}{D_v}\right)}{(S+Zr)} dr = -\Delta t \tag{19}$$

If we integrate Eq.(19), we obtain the following results,

$$\frac{1}{Z^2}\{(S+Z\cdot r)-S\ \ln(S+Z\cdot r)\}_{r_0}^{r_1} + \frac{B}{D_v\cdot Z^3}\left\{\frac{(Zr+S)^2}{2} - 2S\cdot(Zr+S) + S^2\ln(S+Z\cdot r)\right\}_{r_0}^{r_1} = -\Delta t \quad (20)$$

The quadratic relationship in r_1 can be solved by known methods

$$(AA)r_1^2+(BB)r_1+CC=0 \quad (21)$$

where $AA=\frac{Z\cdot B}{2}$

$$BB=-(S\cdot B-Z\cdot D_v)$$

$$CC=-\left\{\left(D_v\cdot S-\frac{B\cdot S^2}{Z}\right)\cdot\ln\ (S+Z\cdot r_1) + (AA)r_0^2+(BB)r_0 - \left(D_v\cdot S-\frac{B\cdot S^2}{Z}\right)\ln(S+Z\cdot r_0) - \Delta t\cdot Z^2\cdot D_v)\right\}$$

Therefore, if we use a generalization of the Newton-Raphson method, we can obtain the final radius of the pore in the above equation.

4.2 Choice of Model Parameters

There are different values of some parameters published in the literature. In order to obtain the results which are appropriate for densification of CANDU fuel, a parametric study was perfo-rmed. Some of the data for the uranium self-diffusion coefficient $D_u=D_v^{th}\times C_0=D_0\times\exp(-Q/RT)$ are summerized in Table 1. Table 2 contains the values used for the present calculations.

Table 1. Uranium Self-Diffusion Coefficient $D_u=D_0\cdot\exp(-Q/RT)$, $R=8.314\ JK^{-1}\ Mol^{-1}$

$D_0(Cm^2\cdot s^{-1})$	Q(KJ. Mol^{-1})	Reference
$4.3\times.10^{-1}$	368	13, 15
0.23	438	13, 16
—	460	13, 17
—	356	13, 18
2.32×10^{-5}	343	6, 19
0.09	444.8	18

Table 2. Values of Parameters

Values	Reference
$D_v^{th}=0.125\ \exp(-222000/RT)cm^2\ sec^{-1}$	1
$D_v^{irr}=10^{-30}\cdot F\ cm^2\cdot sec^{-1}$	13
$D_u=0.09\ \exp(-444800/RT)$	13
r_g=grain radius	—
$R=8.314\ JK^{-1}\ Mol^{-1}$	—
$g=100$	13
$\gamma=6\times10^{-5}\ J\ cm^{-2}$	13
$K=1.38\times10^{-23}\ JK^{-1}$	—
$a=5.47\times10^{-8}cm$	13
$\lambda=6\times10^{-4}cm$	13
$\omega=5\times10^{-19}cm^3$	13
$C_s=0.002$	13, 20

5. Modelling of Fine Pores

As shown in Fig. 4, we assume that inside a UO_2 grain, radius r_g, a population of very fine pores (radius r_p, density Z_p) and a second population of coarse pores(radius r_c, density Z_c) are present. The volume of the fine sized porosity inside a grain, p, is homogeneously distributed within the matrix, where p is given by $p=(4\pi/3)\ r_p^3\ z_p$. Under steady conditions a certain concentration of vacancies in excess of the thermal equilibrium is maintained in the UO_2 matrix because of the continuous input of vacancies from the atomization of the fine pores by fission spikes. Most of the vacancies generated by a single event, they are coalesced to a new pore or they can grow the coarse pore. Because they

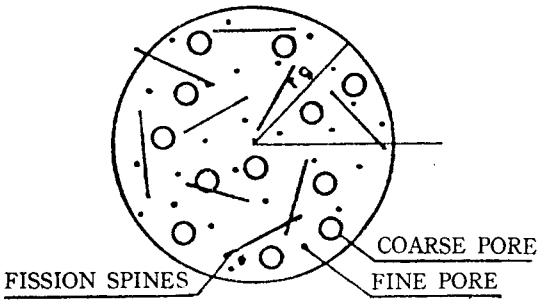

Fig. 4. In-Reactor Densification Model (Fine Pores)

are trapped by coarse pores, only a small fraction of vacancies migrate to the grain boundaries. Nevertheless, because of the large number of vancancies generated by one event and the large number of events per unit time, the contribution of fine pores to the initial densification rate is considerable. Physically, the problem can be treated as a diffusion problem with a homogeneous source of vacancies inside the grain, a densification effective sink at the grain boundary, and ineffective sinks at the surface of the coarse pores inside the grain. So far the disappearance of the very fine pores has been treated only in the high temperature region, i.e., under the assumption that the vacancy diffusion rate is rather and, therefore, the kinetics are purely controlled by the athermal vacancy generation rate(21).

5.1. Dv Rather Large(high temperature), Grain Size Large and Pore Concentration High ($ar_g \ll 1$)

As mentioned in reference (21), the fraction of the vacancies reach the grain boundary, f, is here approximately given by

$$f=\frac{1}{1+(4\pi/3)Z_c r_c r_g/\sqrt{4\pi(Z_c r_c+Z_p r_{p0})}} \tag{22}$$

The densification is therefore

$$\frac{\Delta V}{V_0}=f\,p_0\{1-\exp(-\Omega_{sp}\eta^{**}Ft)\} \tag{23}$$

and

$$\frac{\Delta f_g}{V_0}=(1-f)P_0\ \{1-\exp(-\Omega_{sp}\eta^{**}F\cdot t)\} \tag{24}$$

Hence, in case of well-sintered fuel, coarse pores are grown as much as the amount of $\Delta f_g/V_0$, where Δf_g is the fractional amount of the vacancies absorbed by coarse pore.

5.2. Dv Rather Small (Low temperature approximation, a $r_g \gg 1$)

The average porosity as a function of time follows from

Using the resultant equation in reference (21), the average porosity, $\bar{P}$, is as following Eq.

$$\sqrt{\bar{P}}-\sqrt{P_0}-c_2\ln\frac{\sqrt{\bar{P}}+c_2}{\sqrt{P_0}+c_2}=-\frac{c_1}{2}t \tag{25}$$

(25). If c_2 is a small quantity only, then to a first-order approximation

$$\bar{P}=P_0\left\{1-\frac{3}{2r_g}\sqrt{\frac{\Omega_{sp}\eta C_s D_v}{P_0 F}}\,Ft\right\}^2 \tag{26}$$

The time, t_0, needed for the disapperance of the fine sized porosity is

$$t_0=\frac{2r_g}{3}\sqrt{\frac{P_0}{F\Omega_{sp}\eta C_s D_v}} \tag{27}$$

Eq. (25) and (26) clearly show the influence of the grain size on the densification. Similarly, as shown previously for coarse pore size fractions, the shrinkage is smaller for large grain material than for small grain material. According to the temperature dependence of the vacancy diffusion cofficient, D_v, the pore shrinkage rate depends also on temperature.

6. Comparison with the Experimental Results

For the current version of the KFEDA fuel performance code (22), a densification algorithm which depends on burnup and temperature was developed by fitting to volume-change data from irradiated with Pickering and experimental UO_2 fuels[23] conventionally fabricated with starting densities of 10.2, 10.4, 10.6 and 10.7Mg/m^3. The present densification model is consisted of parameters of which input data are irradiation period, fission rate, pellet temperature and density, pore size distribution, and grain size. In order to calculate the fractions of remaining porosities and to evaluate the results of present model with expermental data, the previous densification algorithm was replaced by the KFMD densification model. And so, the modified KFEDA code uses the initial pore size distribution of Pickering fuel, and then predicts the fuel densifications for Pickering elements as shown in Figs. 5 and 6.

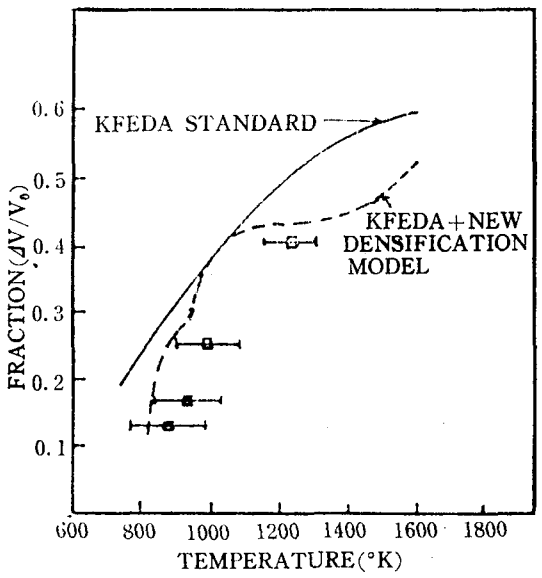

Fig. 5. Fraction of Temperature for Pickering Element No. 10224 Irradiated to 200±15 MWH/KGU

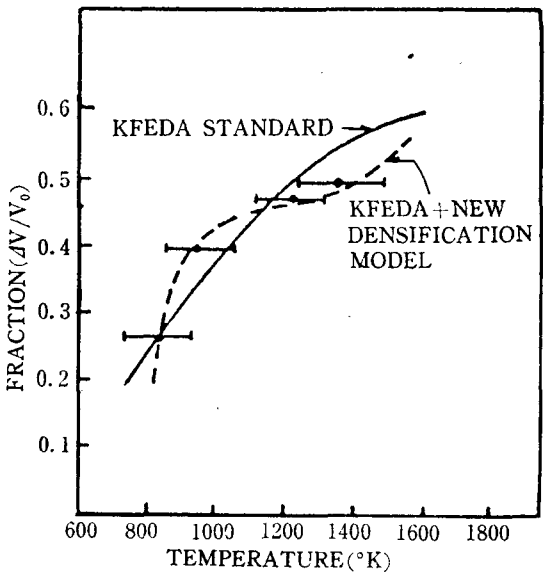

Fig. 6. Fraction ($\Delta V/V_0$) As Function of Temperature for Pickering Element No. 09794 Irradiated to 200±15 MWH/KGU

Figs. 5 and 6 show that the KFEDA densification algorithm predicts the fraction which is monotonically raised with increasing temperature. While, the present densification model predicts the fraction which is a trend in the experimental behaviour. From these figures, it is certainly realized that the present model fits very well with both the absolute magnitute and the temperature variations of the fractions, compared with the KFEDA densification algorithm.

7. Conclusions

The densification model described in this report is based on the Assmann's model. The basic theory relating to the diffusional movement of vacancies in the solids has been presented.

Assmann and Stehle[3] do introduce pore/spike interaction and suggest the rate equation and the relationships for four temperature regimes. Their temperature regimes into which their model is divided are not only observed some discrepancies with experimental data but also there are some discontinuties at the boundaries of each temperature region. To overcome such discrepancies and discontinuties, new integral method of Assmann and Stehle's rate equation is developed and a mechanistic model is proposed to predict nuclear fuel densification.

The present densification model, KFMD, is a function of time, fission rate, temperature, density, pore size distribution and grain size. This model requires the input data of each pore size distribution for each fuel type. The initial pore size distribution is the most important parameter which determines the densification rate. Here, the initial fraction of pores are chracterized by fine pore and coarse pores. In case of coarse pore, it was further characterized by five size ranges. Although this mechanistic modelling seems to need a summation over many pore classes, it is obvious that a subdivision into a few pore classes is sufficient for practical purposes. In order to get the shrinkage rate of corarse pore, the integral method of the rate equation was used in the present work. Bucause each parameter in the rate Eq. (10) has a complica-

ted relation to each other, densification behaviour as shown in this study cannot be defined by any one of these parameters alone and appears to be dependent upon a combination of all of these pellet characteristics.

KFMD mechanistic model provides a simple method of representing changes in pore size spectra during in-reactor densification and total fraction of remaining porosity. As shown in Figs. 5 and 6, both the absolute magnitute and pellet temperature variations of the remained-pore fraction, which resulted from the present model, are agreed very well with the experimental results, comparing with empirical algorithm used in KFEDA. The present mechanistic densification model can be further developed by considering the behaviour of the inter-granular pore which is not yet included.

Reference

1. Dieter Reinfried, "A. Simple Microstructure-Dependent Model for In-reactor Densification of UO_2", Zfk-436, March, 1981.
2. S.R. MacEwen and I.J. Hastings, "A Model for In-rector Densification of UO_2", AECL-4993, September, 1974.
3. M.D. Freshley, D.W. Brite, J.L. Daniel and P.E. Hart, "Irradiation-Induced Densification of UO_2 Pellet Fuel", J. of Nucl. Mat. 62 (1976) p. 138-166.
4. R.L. Coble, J. Appl. Phys. 32 (1961) 787.
5. H. Stehle, H. Assmann and F. Wunderlich, "Uranium Dioxide Properties for LWR/Rods", Nuclear Eng. and Des. 33 (1975) 230-260.
6. M.O. Marlowe, "In-Reactor Densification, Behaviour of UO_2", NEDO-12440, 1973.
7. M.C.J. Carlson, "Densification in Mixed Oxide Fuel During Fast Reactor Irradiation", Nucl. Tech. 22 (1974) 355.
8. H. Zimmermann, "Untersuchungen zum Schwellen und Spaltgasverhalten in Oxidischem Kernbrennestoff unter Neutronenbestrahlung", KFK-2467, 1977.
9. S.R. MacEwen and I.J. Hastings, "A Model for In-Reactor Densification of UO_2", Philosophical Magazine 31 (1975) 135.
10. M.V. Speight, "Point Defects and Irradiation-Enhanced Densification", Philosophical Magazine 32 (1975) 1101.
11. C.C. Dollins and F.A. Nichols, "In-Pile Intragra nular Densification of Oxide Fuels", J. Nucl. Mat. 78 (1978) 326.
12. C.C. Dollins, "In-Pile Densification of Intergranular Porosity in Oxide Fuels", J. Nucl. Mat. 82 (1979) 302.
13. H. Assmann and H. Stehle, "Thermal and In-Reactor Densification of UO_2 Mechanisms and Experimental Results", Nucl. Eng. and Des. 48 (1978) p. 49-67.
14. J.A. Turnbull and R.M. Cornell, "The Resolution of Fission Gas Atoms from Bubbles During the Irradiation of UO_2 at an Elevated Temperature", Jou. of Nucl. Mat. 41 (1971) p. 156-160.
15. A.B. Auskern and J. Belle, "Uranium Ion Self-Diffusion in UO_2", J. Nuclear Material, 3 (1961) p. 267.
16. R. Lindner and F. Schmitz, Diffusion von Uran-233 in Urandioxyd", Z. Naturf. 16a (1961) 1373.
17. Hj. Matzke, "On Uranium Self-Diffusion in UO_2 and Uo_{2+x}" J. Nucl. Mat. 30 (1969) p. 26.
18. J.F. Marin and P. Contamin, "Uranium and Oxygen Self-Diffusion in UO_2", J. Nucl. Mat. 30 (1969) 2f.
19. M.G. Andrews et al., "Evaluating the Solutions to Fuel Densification", Trans. Amer. Nucl. Soc. 19 (1974) 140.
20. G.H. Chalder, P. Dewes and D.B. Scoptt, Paper Presented at Enlarged Halden Program Group Meeting, Sanderstolen, Norway, 7-12, March 1976.
21. H. Stehle and H. Assmann, "In-Reactor UO_2 Densification", Journal of Nucl. Mat. 61 (1976) p. 326-329.
22. Ho Chun Suk et. al., "KFEDA II program description", KAERI/W2/PM-1002-0, 1982.
23. I.J. Hastings and L.E. Evans, "Densification Algorithm for Irradiated UO_2 Fuel", Journal of Ame. Cera., Soc., Vol. 62, No. 3-4, April,

1979.

24. J. Belle, "Uranium Dioxide Properties and Nuclear Application", Naval Reactors, Division of Reactor Development, USAEC, (1961), p. 176.
25. Ho Chun Suk et al, Internal Report, Nuclear Fuel Rod Design Division, KAERI. 1985.